Amphiphilic Polysaccharide Nanoballs: A New Building Block for Nanogel Biomedical Engineering and Artificial Chaperones

Haruko Takahashi,[†,‡] Shin-ichi Sawada,[†] and Kazunari Akiyoshi[†,‡,§,*]

[†]Institute of Biomaterials and Bioengineering, Tokyo Medical and Dental University, 2-3-10 Kanda-Surugadai, Chiyoda-ku, Tokyo, 101-0062, Japan, and [‡]Global Center of Excellence Program for International Research Center for Molecular Science in Tooth and Bone Diseases, Tokyo Medical and Dental University, Japan. [§]Current address: Department of Polymer Chemistry, Graduate School of Engineering, Kyoto University, Katsura, Nishikyo-ku, Kyoto, 615-8510, Japan.

ABSTRACT Enzymatically synthesized glycogen (ESG), a highly branched (1→4)(1→6)-linked α-glucan, is a new monodisperse spherical hyperbranched nanoparticle (molecular weight, 10^6-10^7; diameter, 20−30 nm), polysaccharide nanoball. Amphiphilic ESG nanoballs were synthesized by introducing a cholesterol group to enzymatically synthesized glycogen (CHESG). CHESG assembled into a structure containing a few molecules to form cluster nanogels (approximately 35 nm in diameter) in water. The cluster nanogels were dissociated by the addition of cyclodextrin (CD) to form a supramolecular CHESG−CD nanocomplex due to complexation with the cholesterol group and CD. The CHESG nanogel showed high capacity for complexation with proteins, and the CHESG−CD nanocomplex showed high chaperone-like activity for thermal stabilization of enzymes. CHESG has great potential to become a new building block for nanogel biomedical engineering and to act as an artificial chaperone for protein engineering.

KEYWORDS: enzymatically synthesized glycogen (ESG) · polysaccharide nanoball · nanogel engineering · cyclodextrin · supramolecular complex · protein · artificial chaperone

Enzymatically synthesized glycogen (ESG) is a highly branched (1→4)(1→6)-linked α-glucan that is synthesized from short-chain amylose by cooperative reactions of branching enzyme (BE, EC 2.4.1.18) and amylomaltase (AM, EC 2.4.1.25).[1] ESG is a monodisperse spherical hyperbranched nanoparticle (molecular weight, 10^6-10^7; diameter, 20−30 nm; ≥1000 nonreducing ends), polysaccharide nanoball (Figure 1). In living systems, natural glycogens are found mostly in the liver and skeletal muscle. They act as storage materials to supply glucose to the bloodstream and muscle.[2,3] Differences in the architecture and physicochemical properties between natural glycogens and ESG have been investigated.[4,5] Although ESG has similar properties to natural glycogens, the internal structure is quite different. ESG has a huge α-macrodextrin component as a core, whereas native glycogen has a number of sporadic smaller macromolecules. Because almost all of the α-1,6 linkages of ESG are contained in the large core region, ESG is poorly hydrolyzed by α-amylase, which can usually only degrade the peripheral parts of the ESG molecule. Orally administered ESG has antitumor activity in Meth A tumor-bearing mice,[6] and the safety of oral administration of ESG has been confirmed.[7] Furthermore, immunostimulation of macrophage cells by ESG has also been reported.[8] To our knowledge, however, there are no reports describing the use of ESG as a drug delivery system or in other applications as biomaterials.

Here, we report the synthesis of an amphiphilic ESG nanoball and its characterization as a nanogel. Polysaccharides have been successfully used as key materials for nanomedicine.[9−11] Nanogels have also attracted growing interest as nanocarriers in drug delivery systems.[12,13] We reported previously that pullulan, a linear polysaccharide bearing a small number (<5 mol %) of cholesterol groups (CHP), forms stable nanoparticles in water.[14,15] CHPs behave like hydrated nanometer-sized gels, so-called CHP nanogels, held together via cholesterol nanodomains acting as physical cross-linking points. Other polysaccharides such as mannan and highly branched cyclic dextrin also form nanogels by hydrophobic interaction with cholesterol moieties.[15] CHP nanogels can be complexed with soluble proteins or enzymes[16,17] and exhibit chaperone-like activity.[18,19] These unique properties of nanogels are valuable for their use in protein delivery systems, particularly for cancer vaccines (clinical trials in

*Address correspondence to akiyoshi@bio.polym.kyoto-u.ac.jp.

Received for review June 25, 2010 and accepted November 23, 2010.

Published online December 7, 2010. 10.1021/nn101447m

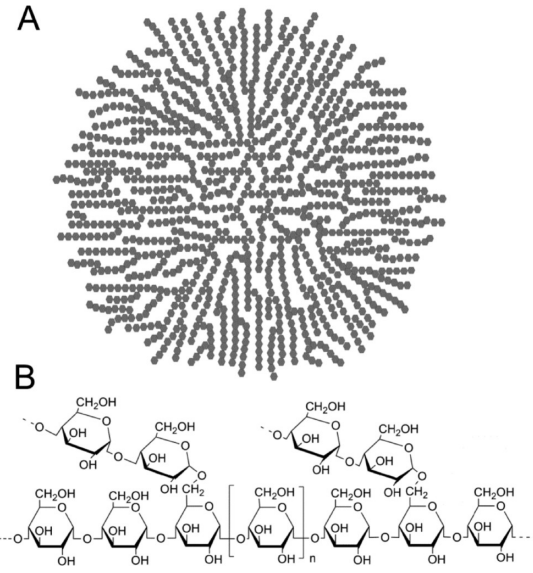

Figure 1. Schematic illustration (A) and chemical structure (B) of ESG.

immunotherapy)[20] and for adjuvant-free intranasal vaccines.[21] Recently, we developed a nanogel bottom-up engineering technique in which polymerizable nanogels are used as building blocks to control the nanostructure of a macrogel.[15] Nanogel cross-linking hydrogels have proven to be useful as a new scaffold material for controlled release in regenerative medicine, including bone regeneration.[15]

In this study, we focused on ESG nanoballs as a new building block for nanogel engineering to design new polysaccharide biomaterials. We synthesized cholesterol group-bearing ESG (CHESG) because cholesterol is the best hydrophobic group for preparation of stable self-assembled nanogels, as previously reported.[14] The solution properties of CHESG in water were investigated using dynamic light scattering (DLS), size-exclusion chromatography (SEC), multiangle laser light scattering (MALS), transmission electron microscopy (TEM), and fluorescence spectroscopy. Interactions with proteins and the artificial chaperone-like activity of CHESG are also described.

RESULTS AND DISCUSSION

Characterization of ESG. ESG used in this study was highly branched (1→4)(1→6)-linked α-glucan in which the percentage of α-1,6 linkages was 8.8% based on ^{1}H NMR estimation. The molecule contained approximately 1400 nonreducing ends and the number-average chain length was 9.3 (calculated as the total number of glucose molecules/number of nonreducing end residues).[1] The molecular weight (M_w) of ESG was 2.2 × 10^6, M_w/M_n = 1.41, and R_G was 11.2 nm by SEC-MALS. The hydrodynamic radius (R_H) measured by DLS was 13.5 ± 0.1 nm and polydispersity index (PDI) calculated by the cumulants analysis was 0.100. The monodispersed spherical nanoparticles were observed by freeze-fracture (FF) TEM (Figure 2A). These results suggested that ESG is a natural dendrimer and monodispersed nanoparticle in the form of a polysaccharide nanoball.

Synthesis and Solution Properties of CHESG. CHESG with varying degrees of substitution (DS) (80, 120, or 140 per one ESG; CHESG80, CHESG120, and CHESG140, respectively) were synthesized by reacting cholesteryl *N*-(6-isocyanatohexyl) carbamate with ESG (Scheme S1 in Supporting Information). These CHESGs easily dissolved in water. The average R_H of CHESGs at an aqueous solution of 1.0 mg/mL was measured by DLS (Table 1) and increased as the DS of the cholesterol group increased (16.1−18.1 nm). The sizes of CHESG stored at 25 °C did not change, even after 20 days, and the particles were colloidally stable (Supporting Information, Figure S1).

The association of CHESGs in a dilute aqueous solution was investigated by SEC-MALS (Table 1). CHESGs formed unimodal multimers with greater molecular weight (M_w = 3.1−6.0 × 10^6, M_w/M_n = 1.11−1.36) than ESG formed (M_w = 2.2 × 10^6, M_w/M_n = 1.41) (the elution profiles are shown in Supporting Information, Figure S2). The data of M_w/M_n

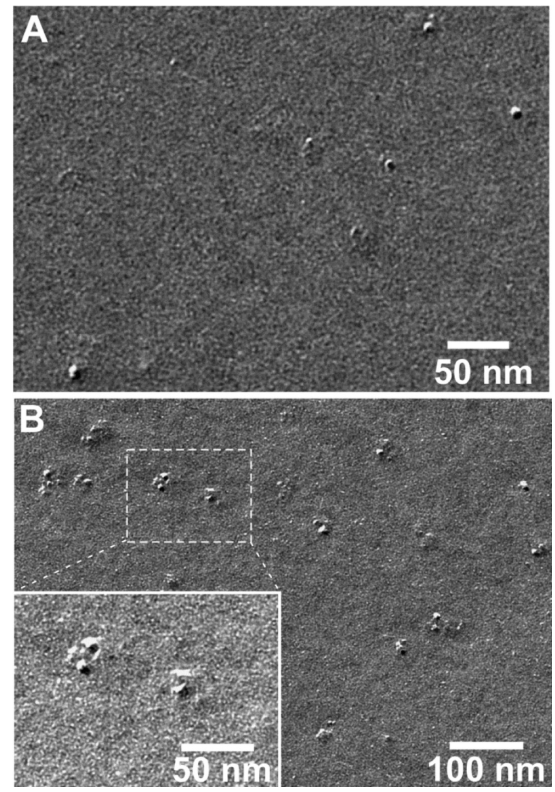

Figure 2. TEM images of ESG (A) and CHESG140 (B).

TABLE 1. Solution Properties of CHESGs

	DS of cholesterol	R_H (nm)	PDI	M_w ($\times 10^6$)	M_w/M_n	N_{CHESG}	Φ_H (g/mL)	N_{ch}	N_{domain}
ESG	0	13.5 ± 0.1	0.100	2.2	1.41		0.370		
CHESG80	80	16.1 ± 0.1	0.114	3.1	1.36	1.4	0.297	28.1 ± 1.5	4.3
CHESG120	120	16.5 ± 0.3	0.079	4.7	1.11	2.2	0.392	31.4 ± 1.6	8.1
CHESG140	140	18.1 ± 0.2	0.081	6.0	1.11	2.7	0.354	22.2 ± 1.2	15.9

(1.1−1.4) and the polydispersity index (PDI) (0.079−0.114) suggested that the nanogels were monodispersive. The number of CHESGs per associate (N_{CHESG}) was calculated from the ratio of the apparent molecular weight of CHESG to ESG. One CHESG self-associate consisted of 1.4−2.7 CHESG molecules in water. The TEM image clearly demonstrates that the CHESG140 formed a cluster nanoparticle with two or three associated CHESG nanoballs (Figure 2B).

The presence of hydrophobic nanodomains in CHESGs was investigated by fluorescence spectroscopy. The I_1/I_3 ratio of the intensity of the emission at 374 nm (I_1) to that of the emission at 385 nm (I_3) for pyrene (Py) spectra is often measured as a probe of the polarity of microenvironment.[22] The ratio has a value of 1.75 when Py is in a polar medium such as water. It is much lower (1.0−1.2) if Py is dissolved in a hydrophobic microenvironment such as the core of surfactant micelles. The emission of Py in a solution of CHESG was around 1.2, consistent with values for Py in a hydrophobic medium (Supporting Information, Figures S3 and S4).

The fluorescence quenching technique is used to determine the aggregation number of surfactant micelles, microdomains of polysoaps, and the cholesterol nanodomains of nanogels.[15] We determined the emission intensity at 384 nm of Py as a function of cetylpyridinium chloride (CPC) concentration, as a fluorescent quencher, in the presence of 8.0−18.0 mg/mL CHESG. The plot of $\ln(I_0/I)$, where I = fluorescence intensity in the presence of a quencher and I_0 = fluorescence intensity in the absence of a quencher, as a function of CPC concentration, showed a good linear relationship across the concentration range (correlation factor, $r > 0.99$) (Supporting Information, Figure S5). Hence, using the slope of the straight line, the mean number of cholesterol moieties in one hydrophobic domain, N_{ch}, can be estimated (see Figure S5).

Table 1 lists the N_{ch} values of various CHESGs obtained using this approach. The CHESG nanogels contained isolated hydrophobic nanodomains (N_{domain}) that were formed by clustering 22−31 cholesterol groups in one nanoparticle. The number of cross-linking points in the nanoparticle increased with an increase in the DS of the cholesterol moiety. The number of cholesterol groups (N_{ch}) in the CHESG (22−31) is higher than that of other nanogels, such as CHP (4−6), cholesterol-bearing mannan, (CHM) (9), and cholesterol-bearing dendritic dextrin (CH-CDex) (11−14).[15] The branching structure of the polysaccharide influences the N_{ch} value of the nanogels. Because CHESGs are high-density nanoparticles with large molecular weights, a large number of cholesterol moieties that easily associate together are found in one nanogel.

The average polymer density (Φ_H) of CHESG obtained from the experimental R_H and M_w values (see experimental section) is up to 0.39 g/mL, indicating that the CHESG nanoparticle consists of, by weight, about 39% polysaccharide and 65% water. The values were comparable to CH−CDex (Φ_H = 026−0.35) but much higher than those of other nanogels such as CHP (Φ_H = 0.16) and CHM (Φ_H = 0.08).[15] In summary, the CHESGs self-assembled into a structure containing a few molecules to form cluster nanogels through physical cross-linking *via* a number of hydrophobic domains in water.

Interactions between CHESG Nanogels and Cyclodextrin (CD). CDs act as solubilizers of various hydrophobic compounds in water by incorporation into hydrophobic cavities. Several CD-based supramolecular materials were recently reported.[23−25] Cholesterol is a suitable guest for β-cyclodextrin (β-CD). When methyl-β-cyclodextrin (M-β-CD) was added to the CHESG nanogels, the size of the CHESGs decreased significantly (13.4 ± 0.1 nm for CHESG80, 13.7 ± 0.1 nm for CHESG120, 14.2 ± 0.1 nm for CHESG140), and reached the R_H of ESG (13.5 ± 0.3 nm). The nanoball cluster of CHESG nanogel dissociated to an ESG monomer because of the loss of hydrophobic interactions between cholesterol groups by complexation with CD (Figure 3). These results support the idea that CHESG self-assembled into a nanocluster through hydrophobic interactions, with cholesterol moieties acting as physical cross-linking points. The complex of CHESG with M-β-CD is also a polysaccharide nanoball that forms an interesting nanosized supramolecule with CD. Thus, CHESG may be a new building block to construct cyclodextrin-based supramolecular nanoarchitectures.

Interactions between CHESG Nanogels and Proteins. We next investigated the interactions between CHESG nanogels and bovine serum albumin (BSA) (M_w = 66 kDa) using a fluorescence probe (tetramethylrhodamine (TAMRA)) and fluorescence correlation spectroscopy (FCS). The percentage of free proteins and bound pro-

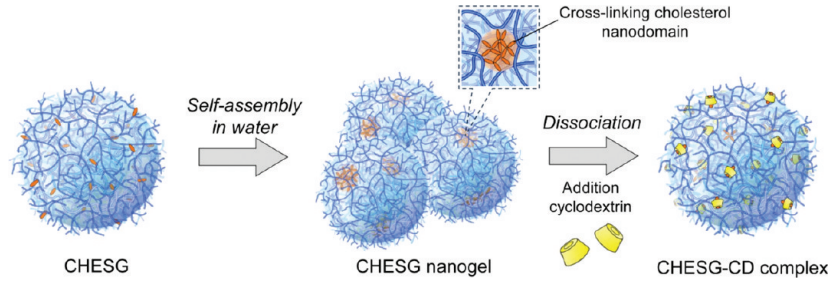

Figure 3. Schematic representation of CHESG association and CD complexation.

teins complexed within the nanogel can be detected by FCS because the diffusion of free TAMRA−BSA is faster than when it is contained in the complex. Figure 4A shows the binding curve for 2.5 nM TAMRA−BSA with CHESG nanogels at increasing nanogel concentrations. CHESG nanogels bound more strongly to TAMRA−BSA than did the ESG bearing an unmodified cholesterol group.

These results suggest that the driving force of protein binding is hydrophobic interactions and the nano-sized network plays an important role. We estimated the binding constants (K) using the assumption that a 1:1 complex is formed under conditions of excess amounts of nanogel over protein. The binding constants were 5.1 ($\pm$3.2) $\times$ 10^7 and 2.5 ($\pm$0.6) $\times$ 10^7 for CHESG120 and CHESG140, respectively. These values were almost comparable with that reported for CHP (1.3 ($\pm$0.2) $\times$ 10^7).[26]

Next, the maximum number of BSA molecules bound to one nanogel was examined by high-performance size exclusion chromatography (HPSEC) (Supporting Information, Figure S6A). Figure 4B shows the numbers of bound BSA molecules per nanogel as a function of time in the presence of an excess concentration of BSA (10 μM) *versus* nanogel (1 μM). Equilibrium was reached after 1 h and the maximum number was approximately five. The value (5 BSA molecules to 1 nanogel molecule) is much higher than that previously reported for CHP nanogels (1 BSA molecule to 1 nanogel molecule).[16] We also repeated this experiment using the smaller protein insulin (M_w = 5.8 kDa) (Supporting Information, Figure S6B). Figure 4B showed that a CHESG nanogel bound 18 insulin molecules. This value is also higher than that previously reported for CHP nanogels (10 insulin molecules to 1 nanogel molecule)[17] and probably is due to the hyper-branched structure of CHESG.

The secondary structure of proteins complexed with the CHESG nanogel was investigated by circular dichroism (cd) measurement (Figure 5). In the CHESG−Ins complex, the cd spectrum changed significantly from the native spectrum similar to CHP or CHCDex nanogels.[15,17] On the other hand, the cd spectrum of the CHESG−BSA complex did not change after com-

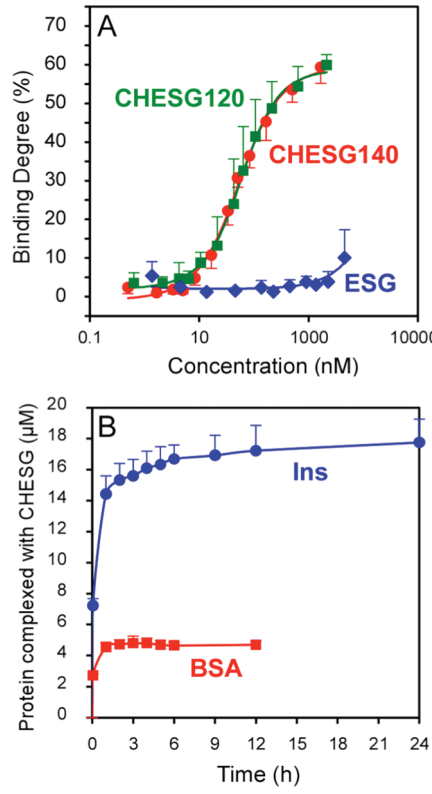

Figure 4. (A) Binding isotherm of TAMRA−BSA (2.5 nM) with ESG, CHESG120 and CHESG140, as estimated by FCS. (B) Complexation of FITC−Ins (30 μM), and FITC−BSA (10 μM) with CHESG140 nanogel (1 μM) as a function of time in PBS (pH 7.4) at 25 °C.

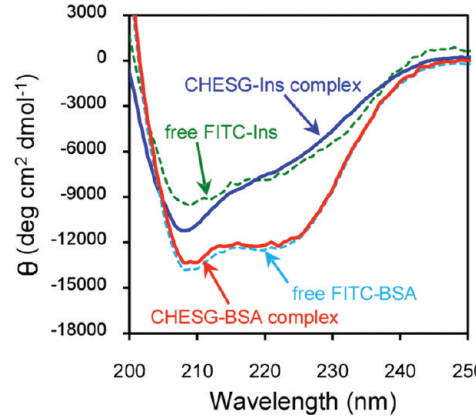

Figure 5. CD spectra of free FITC−Ins, CHESG−Ins complex, free FITC−BSA, and CHESG−BSA complex in PBS (pH 7.4) at 25 °C. [FITC−Ins] = 12 μM, [FITC−BSA] = 4.0 μM, and [CHESG140] = 12.0 mg/mL.

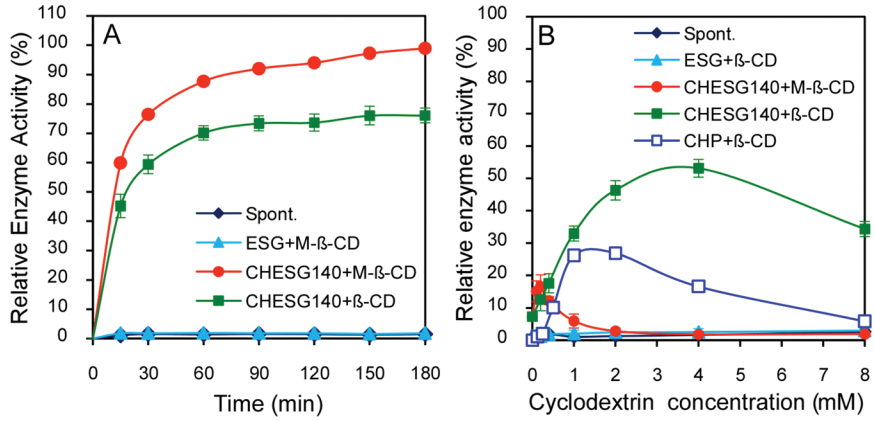

Figure 6. (A) Time-course of recovery of the enzyme activity of CA (2.0 μM) after the addition of CD (4 mM) in the two-step system in 50 mM Tris-sulfate buffer (pH 7.5) at 25 °C. [ESG], [CHESG140] = 6.0 mg/mL. (B) Recovery of enzyme activity of CA (2.0 μM) by the CHESG−cyclodextrin complex as a function of CD concentration in the one-step system in 50 mM Tris-sulfate buffer (pH 7.5) at 25 °C. [ESG], [CHESG140] = 6.0 mg/mL.

plexation, although a drastic change in the cd spectrum for complexed BSA was reported for CHP.[16] The average R_H of the CHESG−Ins complex (19.3 ± 0.3 nm) was similar to that of the parent CHESG140 (18.2 ± 0.2 nm). However, the R_H of the CHESG−BSA complex was 26.9 ± 0.4 nm, much larger than that of CHESG140. Small proteins such as insulin were incorporated inside the CHESG nanogel network and strongly interacted with the hydrophobic domain, which induced conformational changes in Ins. Larger proteins such as BSA associated with the external surface of the CHESG nanogel without significant conformational changes in the protein.

In biological fluids, for example, in blood, there are many proteins such as albumin. The CHESG nanogel should be exposed to excess proteins when the nanogels intravenously injected. We examined the time course of release of FITC−Ins complexed with CHESG nanogel in the presence of excess amount of BSA solution (50 mg/mL) (Supporting Information, Figure S7A, B). In the absence of BSA, FITC−Ins did not release at all at least after 48 h. However, the complexed FITC−Ins was gradually released up to 40% for 48 h in the presence of BSA. After 96 h, 50% of FITC−Ins was still left in the CHESG nanogel. The release of the FITC−Ins was caused by an exchange reaction with BSA as previously reported.[15] FITC-labeled insulins incorporated deeply inside the nanogel network may not be easily released from the complex.

The CHESG Nanogel−CD System as an Artificial Chaperone. Most proteins irreversibly aggregate upon heating. In living systems, molecular chaperones, such as the GroEL−GroES system, selectively trap heat-denatured proteins, primarily *via* hydrophobic interactions, to prevent their irreversible aggregation.[27,28] The host chaperone releases the guest protein in a refolded form through a change in the conformation of the complex with the aid of ATP. Molecular chaperone systems inspired us to explore new approaches for thermal stabilization of proteins.[23,29−37] Previously, we investigated the heat shock protein-like activity (thermal stabilization) of a CHP nanogel−CD system for enzymes such as carbonic anhydrase (CA) and citrate synthase (CS).[18,19]

The heat shock protein-like activity of the CHESG nanogel was investigated using carbonic anhydrase II (CA) from bovine erythrocytes as a model protein. CA is a monomeric enzyme (M_w = 30 kDa) that contains zinc in its active center and does not have a disulfide bridge. CA was heated at 70 °C for 10 min and cooled to room temperature. The enzyme activity was completely lost as a result of the aggregation of heat-denatured CA. However, in the presence of CHESG nanogel under the same conditions, the enzyme activity recovered after the addition of M-β-CD (recovery % > 95%) and β-CD (75%) (Figure 6A).

The complexation of carbonic anhydrase II (CA) with CHESG nanogel was investigated using HPSEC. The CHESG nanogel (1.0 μM) was incubated with excess CA (20 μM) at 25 °C for 24 h or 75 °C for 10 min. Native CA did not complex so much with CHESG nanogel under incubation at 25 °C even for 24 h (Supporting Information, Figure S8). On the other hand, heat-denatured CA significantly bound to CHESG nanogel only for 10 min. The CHESG nanogel selectively interacted with heat-denatured CA (Figure S8). This is similar to the function of a natural molecular chaperone.

The irreversible aggregation of CA upon heating was completely prevented by complexation between the heat-denatured enzyme and the CHESG nanogel. The complexed CA was then released after removal of the hydrophobic interactions with the cholesterol group of CHESG upon the addition of β-CD. The released CA refolded into its native form (Supporting Information, Figure S9). The differences between the chaperone-like activities of β-CD and M-β-CD can be attributed to differences in their binding ability for the cholesterol group. The interaction of CHESG nanogel

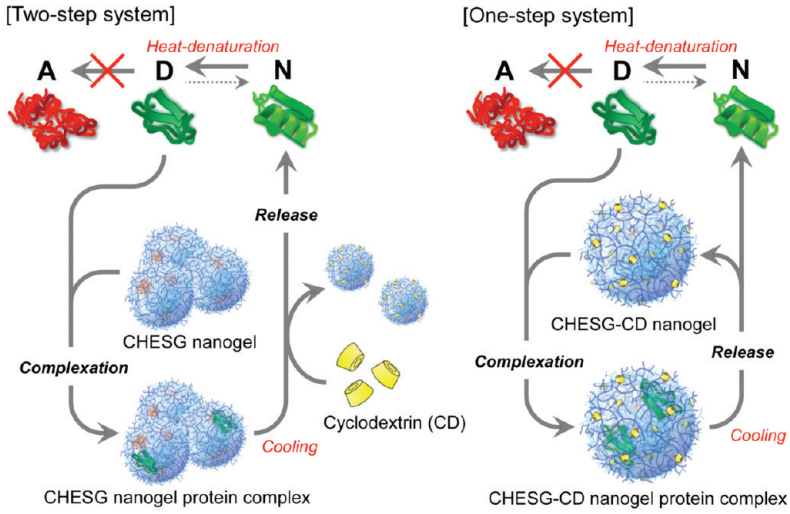

Figure 7. Schematic representation of the artificial chaperone activity of the CA−CHESG system (two-step system) and the CHESG−CD supramolecular system (one-step system).

with β-CD and M-β-CD was investigated by DLS. The sizes of CHESG in the presence of various concentrations of methyl-β-CD or β-CD were measured (Figure S10). The size of CHESG nanogel decreased by the addition of methyl-β-CD up to the size of unmodified ESG. This means that the nanogel cluster effectively dissociated to the CHESG−CD complex. In the case of addition of β-CD, the size of CHESG did not reach the size of unmodified ESG. The nanogel cluster with CHESG−CD complex still remained due to weaker interaction of β-CD with cholesterol than that of methyl-β-CD. The differences of the interaction affect the chaperon-like activity of the CHESG nanogel. M-β-CD effectively complexed and released the protein from the nanogels. Using the CHESG−M-β-CD system, it was possible to recover 90% of the activity of three CA enzymes for every one CHESG nanogel molecule. The CHESG nanogel achieved high refolding efficiency compared with the CHP−M-β-CD system, which allowed only one CA per one nanogel.

The CHESG−CD Supramolecular System as an Artificial Chaperone. The capture and release of proteins by the nanogel−CD system mentioned above are sequential and separate processes that essentially occur in two steps. However, in a molecular chaperone system, the two processes periodically and dynamically proceed concurrently in the presence of ATP and a cochaperone.[27,28] We previously reported a chaperone-like function of a host−guest complex of CHP and CD.[19] The dynamic nanogels of CHP−CD self-regulated the association of heat-denatured protein and dissociation of native protein depending on the concentration of CD. These CHP−CD nanogels showed heat shock protein-like activity acting as a concurrent artificial molecular chaperone system. Therefore, we investigated the possible concurrent chaperone-like activity of the CHESG−CD complex as a supramolecular nanoball in a one-step system.

The recovery of enzyme activity after heating at 70 °C for 10 min was examined in the presence of the CHESG−CD complex. The CHESG−CD complex at various concentrations of CD was prepared by co-incubation for 1 h. Then CA was added to the solution and the mixture was heated at 70 °C for 10 min. After the solution was cooled for 24 h, the residual enzyme activity was measured (Figure 6B). In the CHESG−CD system, the chaperone-like activity varied significantly, depending on whether β-CD or M-β-CD was used. The nanogel−CD supramolecular system appeared to act as a hydrophobic buffer by blocking the exposed hydrophobic surface on the heat-denatured protein, just enough to prevent aggregation. On the other hand, physically weak binding to the denatured proteins would not prevent their aggregation while physically strong binding to the protein would prevent refolding to the native conformation. Thus, a delicate balance is required for higher thermal stabilization of the protein. Since every protein has various denatured conformations with different hydrophobic and hydrophilic properties, chaperones should be capable of adjusting the various protein conformations appropriately to achieve higher activity. We were able to control the hydrophobic−hydrophilic balance and also the nano-sized network inside the nanoballs by changing the type of CDs used and their concentration.

It is noteworthy that the CHESG−β-CD supramolecular system, as illustrated in Figure 7, showed much higher chaperone-like activity than the CHP−β-CD system. The low efficiency of the CHP−β-CD system was probably due to the loss of the three-dimensional structure of the CHP nanogel after complexation with CD. Although the CHESG nanogel clusters dissociated in the presence of CD, they still formed a three-dimensional nanoarchitecture based on the results with the ESG hyperbranched nanoball (Supporting Information, Figure S11). The three-dimensional structure would offer an effective space to prevent the aggregation of denatured proteins and for refolding the proteins. Thus, CHESG has significant potential as an artificial molecular chaperone for protein engineering.

CONCLUSIONS

Cholesterol group-modified ESG (a hydrophobic polysaccharide nanoball) formed cluster nanogels, approximately 35 nm in diameter, *via* a number of hydrophobic domains as physical cross-linking points. The CHESG nanogel was capable of strong complexation with a number of proteins and the CHESG−CD supramolecular system showed high chaperone-like activ-

ity for thermal stabilization of enzymes. These functions are valuable for protein engineering or protein delivery systems. ESG nanoball-based materials should offer new opportunities as building blocks for nanogel engineering for medical, pharmaceutical, and cosmetic applications.

EXPERIMENTAL SECTION

Materials. Enzymatically synthesized glycogen (ESG) (M_w = 2.20 × 10^6, M_w/M_n = 1.41) was a kind gift from EZAKI GLICO Co., Ltd. (Osaka, Japan). TAMRA−BSA, fluorescein isothiocyanate (FITC)-labeled insulin (FITC−Ins), FITC-labeled BSA (FITC−BSA) and CA from bovine erythrocytes were purchased from Sigma-Aldrich, Inc. (Saint Louis, MO). TAMRA−BSA and FITC−BSA were used after purification. All other reagents were commercially available and were used without further purification.

Synthesis of CHESG. CHESG was synthesized according to a previously described method.[14] In brief, ESG in dry dimethyl sulfoxide (DMSO) was reacted with cholesteryl *N*-(6-isocyanatohexyl)carbamate in dry pyridine at 80 °C for 8 h. The reaction solution was dropped into excess ether/ethanol (ether > 85%), and the precipitates were washed with ether/ethanol. The precipitates were then dissolved in DMSO again, dialyzed against distilled water, and lyophilized to give a white powder. The DS of the cholesterol group was determined by ^{1}H NMR. ^{1}H NMR (DMSO-d6/D_2O = 9/1 (v/v)): σ 0.4−1.9 (51H, cholesterol group), 2.8−4.6 (glucose, 2H, 3H, 4H, 5H, and 6H), 4.9−5.5 (glucose, 1H(1→4)). CHESG containing 80, 120, or 140 cholesterol groups per one ESG molecule (CHESG80, CHESG120 and CHESG140, respectively), were obtained.

Preparation of CHESG Solutions. CHESG was dissolved in phosphate-buffered saline (Dulbecco's PBS, pH 7.4, Sigma) or 50 mM Tris-sulfate buffer (pH 7.5) with stirring to give a clear solution. The solution was sonicated at 40 W for 15 min with a sonicator probe (Sonifier 250, Branson Ultrasonics Co., Danbury, CT) and filtered through a 0.22-μm PVDF filter (Millex-GV, Millipore Co., Bedford, MA).

FF-TEM. FF-TEM observations of replicas of samples were performed using a TEM (JEM-1011, JEOL, Tokyo, Japan) at an accelerating voltage of 100 kV. To prepare the replicas, CHESG was suspended at a concentration of 14.0 mg/mL in Milli-Q water containing 30% glycerin, and then freeze-fractured mechanically. The fracturing and replication were carried out on a FF device (JFD-9010, JEOL, Tokyo, Japan) at −120 °C and 10^{-5} Pa.

DLS Measurements. DLS measurements were carried out at 25 °C using a Zetasizer Nano ZS (Malvern Instruments Ltd., Malvern, Worcestershire, UK) at a wavelength of 633 nm and a 173° detection angle to determine the size of the CHESG nanogels. DLS measurements of the CHESG nanogel solutions were performed in the absence or presence of M-β-CD. CHESG was suspended at a concentration of 1.0 mg/mL in PBS. Then, 300 mM of M-β-CD was added to the CHESG solution (1/10 (v/v)) and mixed at 25 °C for 3 h. The measured autocorrelation function was analyzed by the cumulant method. The hydrodynamic radius of the particles was calculated using the Stokes−Einstein equation.

SEC-MALS. The SEC-MALS system consisted of a RI-8020 refractive index detector (Tosoh Co., Tokyo, Japan), and a DAWN-DSP MALS detector with a laser operated at 690 nm (Wyatt Technology, Santa Barbara, CA), using a SEC column (Sephacryl S-500, GE Healthcare, Φ10 mm ×300 mm) eluted with PBS (pH 7.4, Sigma) at a flow rate of 0.4 mL/min at 25 °C. Molecular weights and molecular weight distributions were calculated using ASTRA software (Wyatt Technology, Santa Barbara, CA) based on Zimm's equation with a refractive index increment (d*n*/d*c*) of 0.149 mL/g (determined experimentally).

From the experimental R_H and M_w values, an average polymer density (Φ_H) within a CHESG nanoparticle was calculated according to

$$\Phi_H = \left(\frac{M_w}{N_A}\right)\left(\frac{4}{3}\pi R_H^3\right)^{-1} \quad (1)$$

where N_A is Avogadro's number.

FCS. The binding constants of BSA with the CHESG nanogels were estimated by FCS, as previously described.[26] FCS measurements were performed using FluoroPoint-Light software (Olympus Co., Tokyo, Japan). Various concentrations of the CHESG solutions were mixed with TAMRA−BSA (final concentration 2.5 nM), and these mixtures were incubated at 25 °C for 24 h. All experiments were performed with an acquisition time of 10 s per measurement, with triplicate measurements per sample. The FCS data were analyzed using FluoroPoint-Light software. The binding constants were calculated from triplicate measurements with an Origin 8 (OriginLab Co., Northampton, MA) using best fit. The protein-binding reaction to nanogel was represented by

$$\text{protein} + \text{nanogel} \rightleftarrows \text{complex} \quad (2)$$

The binding constant K can be evaluated according to the following equations:

$$K = \frac{1}{K_d} \quad (3)$$

$$K_d = \frac{[A][B]}{[AB]} \quad (4)$$

$$Y = \frac{K_d + [A] + [B] - \sqrt{(K_d + [A] + [B])^2 - 4[A][B]}}{2[A]} \quad (5)$$

Where K_d is the dissociation constant, [A] and [B] are the molar concentrations of TAMRA−BSA and CHESG, respectively, and Y is the degree of complexation of TAMRA−BSA and CHESG in the solution.

Complexation of Proteins with CHESG Nanogels. The complexation number of proteins with CHESG was measured by HPSEC (Shimadzu Co., Kyoto, Japan), which consisted of a LC-20AT pump, a RID-10A refractive index detector, and a SPD-20A UV detector. We used a Superose 12 10/300 GL column (GE Healthcare, Φ10 mm × 300 mm) eluted with PBS (pH 7.4, Sigma) at a flow rate of 0.5 mL/min at 25 °C. CHESG was suspended at a concentration of 12.0 mg/mL (2.0 μM) in PBS; 60 μM of FITC−Ins or 20 μM of FITC−BSA was added to the CHESG solution, and incubated at 25 °C. The final concentration of CHESG was 1.0 μM, that of FITC−Ins was 30 μM, and that of FITC−BSA was 10 μM. At a given interval, an aliquot (20 μL) was injected to the HPSEC. The amount of protein complexation was determined by UV detection at 494 nm. The complexed protein concentration (μM) was calculated from the area-concentration standard curve prepared by peak areas of free protein at various concentrations.

Circular Dichroism (cd) Measurements. The cd spectra were measured using a quartz cuvette and a JASCO J-720 spectropolarimeter under a constant gaseous nitrogen flow at 25 °C. CHESG was suspended at a concentration of 24.0 mg/mL (4.0 μM) in PBS. Then, 48 μM of FITC−Ins or 8.0 μM of FITC−BSA was added to the CHESG solution and incubated at 25 °C. The final concentration of CHESG was 2.0 μM, that of FITC−Ins was 12 μM, and that of FITC−BSA was 4.0 μM. After incubation (3 h for FITC−Ins or 24 h for FITC−BSA), the cd spectra were measured.

Chaperone-like Activity of the CHESG Nanogel−CD System (Two-Step System). CHESG was suspended at a concentration of 6.1 mg/mL (1.0 μM) in 50 mM Tris-sulfate buffer (pH 7.5). Native CA was dissolved at a concentration of 3.0 mg/mL (100 μM) in 50 mM Tris-sulfate buffer and was rapidly diluted 50-fold by the CHESG solution. The final concentration of CHESG was 1.0 μM and that of CA was 2.0 μM. The mixture was then heated at 70 °C for 10 min, and cooled to room temperature for 1 h. Finally, β-CD or M-β-CD was added to a final concentration of 4.0 mM and mixed gently. At a given interval, the recovery of the enzyme activity of heat-denatured CA was determined by a *p*-nitrophenyl ac-

etate (*p*NPA) hydrolysis assay.[18,19] A 50 μL portion of a dry acetonitrile solution of 50 mM *p*NPA was added to 450 μL of the sample solution. After mixing for 5 s, an increase in the *p*-nitrophenolate concentration was monitored by the absorbance at 400 nm as a function of time using a V-660 spectrophotometer (JASCO Co., Tokyo, Japan). The percent recovery of enzyme activity was calculated on the basis of the initial activity of native CA. The protein concentration of native CA was determined by absorbance at 280 nm with a coefficient of 1.83 mg protein/mL/cm.

Chaperone-like Activity of the CHESG−CD Supramolecular Complex (One-Step System). CHESG was suspended at a concentration of 6.1 mg/mL in 50 mM Tris-sulfate buffer. Various concentrations of β-CD or M-β-CD were added to the CHESG solution and incubated at 25 °C for 1 h to obtain the CHESG−CD complex solution. Native CA was dissolved at a concentration of 3.0 mg/mL (100 μM) in 50 mM Tris-sulfate buffer and was rapidly diluted by 50-fold in the CHESG−CD complex solution to achieve a final concentration of CA of 0.06 mg/mL (2.0 μM). The mixture was heated at 70 °C for 10 min and then cooled to 25 °C. After incubation at 25 °C for 24 h, the enzyme activity was measured using the aforementioned *p*NPA hydrolysis assay.

Acknowledgment. The authors thank Dr. Hiroki Takata and Dr. Takeshi Takaha, Institute of Health Sciences, Ezaki Glico Co., Ltd. for the kind gift of ESG and for helpful discussions. This work was supported by a Grant-in-Aid for Scientific Research from the Ministry of Education, Culture, Sports, Science and Technology (Grant No. 20240047 and No. 18GS0421).

Supporting Information Available: Synthesis of CHESG; fluorescence measurements; additional figures. This material is available free of charge *via* the Internet at http://pubs.acs.org.

REFERENCES AND NOTES

1. Kajiura, H.; Kakutani, R.; Akiyama, T.; Takata, H.; Kuriki, T. A Novel Enzymatic Process for Glycogen Production. *Biocatal. Biotransform.* **2008**, *26*, 133–140.
2. Geddes, R. Glycogen: A Metabolic Viewpoint. *Biosci. Rep.* **1986**, *6*, 415–428.
3. Smythe, C.; Cohen, P. The Discovery of Glycogenin and the Priming Mechanism for Glycogen Biogenesis. *Eur. J. Biochem.* **1991**, *200*, 625–631.
4. Takata, H.; Kajiura, H.; Furuyashiki, T.; Kakutani, R.; Kuriki, T. Fine Structural Properties of Natural and Synthetic Glycogens. *Carbohydr. Res.* **2009**, *344*, 654–659.
5. Kajiura, H.; Takata, H.; Kuriki, T.; Kitamura, S. Structure and Solution Properties of Enzymatically Synthesized Glycogen. *Carbohydr. Res.* **2010**, *345*, 817–824.
6. Ryoyama, K.; Kidachi, Y.; Yamaguchi, H.; Kajiura, H.; Takata, H. Anti-Tumor Activity of an Enzymatically Synthesized α-1,6 Branched α-1,4-Glucan, Glycogen. *Biosci. Biotechnol. Biochem.* **2004**, *68*, 2332–2340.
7. Tafazoli, S.; Wong, A. W.; Kajiura, H.; Kakutani, R.; Furuyashiki, T.; Takata, H.; Kuriki, T. Safety Evaluation of an Enzymatically-Synthesized Glycogen (ESG). *Regul. Toxicol. Pharmacol.* **2010**, *57*, 210–219.
8. Kakutani, R.; Adachi, Y.; Kajiura, H.; Takata, H.; Kuriki, T.; Ohno, N. Relationship between Structure and Immunostimulating Activity of Enzymatically Synthesized Glycogen. *Carbohydr. Res.* **2007**, *342*, 2371–2379.
9. Liu, Z.; Jiao, Y.; Wang, Y.; Zhou, C.; Zhang, Z. Polysaccharides-based Nanoparticles as Drug Delivery Systems. *Adv. Drug Delivery Rev.* **2008**, *60*, 1650–1662.
10. Park, K.; Lee, S.; Kang, E.; Kim, K.; Choi, K.; Kwon, I. C. New Generation of Multifunctional Nanoparticles for Cancer Imaging and Therapy. *Adv. Funct. Mater.* **2009**, *19*, 1553–1566.
11. Mao, S.; Sun, W.; Kissel, T. Chitosan-Based Formulations for Delivery of DNA and siRNA. *Adv. Drug Delivery* **2010**, *62*, 12–27.
12. Kabanov, A. V.; Vinogradov, S. V. Nanogels as Pharmaceutical Carriers: Finite Networks of Infinite Capabilities. *Angew. Chem., Int. Ed.* **2009**, *48*, 5418–5429.
13. Raemdonck, K.; Demeester, J.; Smedt, S. D. Advanced Nanogel Engineering for Drug Delivery. *Soft Matter* **2009**, *5*, 707–715.
14. Akiyoshi, K.; Deguchi, S.; Moriguchi, N.; Yamaguchi, S. Sunamoto. Self-Aggregates of Hydrophobized Polysaccharides in Water. Formation and Characteristics of Nanoparticles. *J. Macromolecules* **1993**, *26*, 3062–3068.
15. Sasaki, Y.; Akiyoshi, K. Nanogel Engineering for New Nanobiomaterials: From Chaperoning Engineering to Biomedical Applications. *Chem. Rec.* **2010**, *10*, 366−376.
16. Nishikawa, T.; Akiyoshi, K.; Sunamoto, J. Macromolecular Complexation between Bovine Serum Albumin and the Self-Assembled Hydrogel Nanoparticle of Hydrophobized Polysaccharides. *J. Am. Chem. Soc.* **1996**, *118*, 6110–6115.
17. Akiyoshi, K.; Kobayashi, S.; Shichibe, S.; Mix, D.; Baudys, M.; Kim, S. W.; Sunamoto, J. Self-Assembled Hydrogel Nanoparticle of Cholesterol-Bearing Pullulan as a Carrier of Protein Drugs: Complexation and Stabilization of Insulin. *J. Controlled Release* **1998**, *54*, 313–320.
18. Akiyoshi, K.; Sasaki, Y.; Sunamoto, J. Molecular Chaperone-like Activity of Hydrogel Nanoparticles of Hydrophobized Pullulan: Thermal Stabilization with Refolding of Carbonic Anhydrase B. *Bioconjugate Chem.* **1999**, *10*, 321–324.
19. Nomura, Y.; Sasaki, Y.; Takagi, M.; Narita, T.; Aoyama, Y.; Akiyoshi, K. Thermoresponsive Controlled Association of Protein with a Dynamic Nanogel of Hydrophobized Polysaccharide and Cyclodextrin: Heat Shock Protein-like Activity of Artificial Molecular Chaperone. *Biomacromolecules* **2005**, *6*, 447–452.
20. Tsuji, K.; Hamada, T.; Uenaka, A.; Wada, H.; Sato, E.; Isobe, M.; Asagoe, K.; Yamasaki, O.; Shiku, H.; Ritter, G.; Murphy, R.; Hoffman, E. W.; Old, L. J.; Nakayama, E.; Iwatsuki, E. Induction of Immune Response Against NY-ESO-1 by CHP-NY-ESO-1 Vaccination and Immune Regulation in a Melanoma Patient. *Cancer Immunol. Immunother.* **2008**, *57*, 1429–1437.
21. Nochi, T.; Yuki, Y.; Takahashi, H.; Sawada, S.; Mejima, M.; Kohda, T.; Harada, N.; Kong, II. G.; Sato, A.; Kataoka, N.; Tokuhara, D.; Kurokawa, S.; Takahashi, Y.; Tsukada, H.; Kozaki, S.; Akiyoshi, K.; Kiyono, H. Nanogel Antigenic Protein-Delivery System for Adjuvant-free Intranasal Vaccines. *Nat. Mater.* **2010**, *9*, 572–578.
22. Colombani, O.; Ruppel, M.; Schubert, F.; Zettl, H.; Pergushov, D. V.; Müller, A. H. E. Synthesis of Poly(*n*-butyl acrylate)-*block*-poly(acrylic acid) Diblock Copolymers by ATRP and Their Micellization in Water. *Macromolecules* **2007**, *40*, 4338–4350.
23. Villalonga, R.; Cao, R.; Fragoso, A. Supramolecular Chemistry of Cyclodextrins in Enzyme Technology. *Chem. Rev.* **2007**, *107*, 3088–3116.
24. Davis, M. E. The First Targeted Delivery of siRNA in Humans *via* a Self-Assembling, Cyclodextrin Polymer-Based Nanoparticle: From Concept to Clinic. *Mol. Pharm.* **2009**, *6*, 659–668.
25. Manakker, F.; Vermonden, T.; Nostrum, C. F.; Hennink, W. E. Cyclodextrin-Based Polymeric Materials: Synthesis, Properties, and Pharmaceutical/Biomedical Applications. *Biomacromolecules* **2009**, *10*, 3157–3175.
26. Ayame, H.; Morimoto, N.; Akiyoshi, K. Self-Assembled Cationic Nanogels for Intracellular Protein Delivery. *Bioconjugate Chem.* **2008**, *19*, 882–890.
27. Hartl, F. U. Molecular Chaperones in Cellular Protein Folding. *Nature* **1996**, *381*, 571–580.
28. Taguchi, H.; Ueno, T.; Tadakuma, H.; Yoshida, M.; Funatsu, T. Single-Molecule Observation of Protein−Protein Interactions in the Chaperonin System. *Nat. Biotechnol.* **2001**, *19*, 861–865.
29. Rozema, D; Gellman, S. H. Artificial Chaperone-Assisted Refolding of Carbonic Anhydrase B. *Biol. Chem* **1996**, *271*, 3478–3487.
30. Machida, S.; Ogawa, S.; Xiaohua, S.; Takaha, T.; Fujii, K.; Hayashi, K. Cycloamylose as an Efficient Artificial Chaperone for Protein Refolding. *FEBS Lett.* **2000**, *486*, 131–135.
31. Mannen, T.; Yamaguchi, S.; Honda, J.; Sugimoto, S.;

Nagamune, T. Expanded-Bed Protein Refolding Using a Solid-Phase Artificial Chaperone. *J. Biosci. Bioeng.* **2001**, *91*, 403–408.
32. Lanckriet, H.; Middelberg, A. P. J. Operational Regimes for a Simplified One-Step Artificial Chaperone Refolding Method. *Biotechnol. Prog.* **2004**, *20*, 1861–1867.
33. Lu, D.; Zhang, K.; Liu, Z. Protein Refolding Assisted by an Artificial Chaperone Using Temperature Stimuli Responsive Polymer as the Stripper. *Biochem. Eng. J.* **2005**, *25*, 141–149.
34. Swietnicki, W. Folding Aggregated Proteins into Functionally Active Forms. *Curr. Opin. Biotech.* **2006**, *17*, 367–372.
35. Toda, M.; Itoh, H.; Kondo, Y.; Hamada, F. HSP90-like Artificial Chaperone Activity Based on Indole β-Cyclodextrin. *Bioorg. Med. Chem.* **2007**, *15*, 1983–1988.
36. Yazdanparast, R.; Esmaeili, M. A.; Khodagholi, F. Control of Aggregation in Protein Refolding: Cooperative Effects of Artificial Chaperone and Cold Temperature. *Int. J. Biol. Macromol.* **2007**, *40*, 126–133.
37. Sasaki, Y.; Akiyoshi, K. Development of an Artificial Chaperone System Based on Cyclodextrin. *Curr. Pharm. Biotechnol.* **2010**, *11*, 300–305.